Development 136, 855-864 (2009) doi:10.1242/dev.028605

EphA4 as an effector of *Twist1* in the guidance of osteogenic precursor cells during calvarial bone growth and in craniosynostosis

Man-Chun Ting, Nancy L. Wu, Paul G. Roybal, Jingjing Sun, Liqiong Liu, Youzhen Yen and Robert E. Maxson, Jr*

Heterozygous loss of *Twist1* function causes coronal synostosis in both mice and humans. We showed previously that in mice this phenotype is associated with a defect in the neural crest-mesoderm boundary within the coronal suture, as well as with a reduction in the expression of ephrin A2 (*Efna2*), ephrin A4 (*Efna4*) and *EphA4* in the coronal suture. We also demonstrated that mutations in human *EFNA4* are a cause of non-syndromic coronal synostosis. Here we investigate the cellular mechanisms by which *Twist1*, acting through Eph-ephrin signaling, regulates coronal suture development. We show that *EphA4* mutant mice exhibit defects in the coronal suture and neural crest-mesoderm boundary that phenocopy those of *Twist1*$^{+/-}$ mice. Further, we demonstrate that *Twist1* and *EphA4* interact genetically: *EphA4* expression in the coronal suture is reduced in *Twist1* mutants, and compound *Twist1-EphA4* heterozygotes have suture defects of greater severity than those of individual heterozygotes. Thus, *EphA4* is a *Twist1* effector in coronal suture development. Finally, by DiI labeling of migratory osteogenic precursor cells that contribute to the frontal and parietal bones, we show that *Twist1* and *EphA4* are required for the exclusion of such cells from the coronal suture. We suggest that the failure of this process in *Twist1* and *EphA4* mutants is the cause of craniosynostosis.

KEY WORDS: EphA4, Twist1, Boundary formation, Cell guidance, Craniosynostosis

INTRODUCTION

The patterned growth of organ rudiments depends on the close regulation of cell proliferation, differentiation and migration. Defining the contributions of these processes is key to understanding how pattern is established, and how developmental anomalies arise. Here we address the cellular mechanisms that control the growth of the mammalian skull vault, as well as the mechanisms underlying craniosynostosis, the premature fusion of the calvarial bones.

The mammalian skull vault is a composite structure, consisting of membrane bones with distinct lineage origins (Jiang et al., 2002). The frontal bones and the central portion of the interparietal bone are derived from neural crest, the parietal bones and the lateral portion of the interparietal bone from paraxial mesoderm. The bones of the skull vault are separated by sutures, fibrous joints that accommodate the expanding brain and allow the skull to undergo reshaping during birth. Craniosynostosis, the premature fusion of calvarial bones at the sutures, occurs as frequently as 1 in 2500 live births. Affected individuals have abnormally shaped skulls, and in some instances mental retardation and impaired vision and hearing (Cohen and MacLean, 1999; Wilkie and Morriss-Kay, 2001).

Mutations in a number of genes, collectively functioning in several signaling pathways, can cause craniosynostosis in humans or mice (Ornitz and Marie, 2002; Rawlins and Opperman, 2008; Wilkie, 1997). Among these genes are *TWIST1*, which regulates both BMP and FGF signaling (Carver et al., 2002; Connerney et al., 2008; el Ghouzzi et al., 1997; Howard et al., 1997; Rice et al., 2000; Rice et al., 1999; Wilkie, 1997), *FGFR1*, *FGFR2* and *FGFR3* (Jabs et al., 1994; Marie et al., 2005; Meyers et al., 1995; Yu et al., 2003), the Wnt pathway inhibitor, *Axin2* (Yu et al., 2005), the Bmp target, *MSX2* (Jabs et al., 1993), and *RAB23*, a component of the Shh pathway (Jenkins et al., 2007). The cellular mechanisms underlying craniosynostosis have been investigated using both mouse and tissue culture models (Maxson and Ishii, 2008; Rawlins and Opperman, 2008; Wilkie and Morriss-Kay, 2001). Mice carrying the S252W or P253R mutation engineered into Fgfr2 mimic features of Apert syndrome (Wang et al., 2005; Yin et al., 2008), and exhibit enhanced RTK signaling (Shukla et al., 2007). Activation of Wnt signaling by targeted deletion of *Axin2* results in an expansion of the pool of osteoprogenitors and ultimately to synostosis (Liu et al., 2007; Yu et al., 2005). Although details of underlying developmental mechanisms that lead ultimately to synostosis are still lacking, one reasonable hypothesis is that it is caused by changes in the balance of proliferation and differentiation of osteogenic cells in the developing suture (Bialek et al., 2004; Chen et al., 2003; Lee et al., 1999; Yousfi et al., 2002; Yousfi et al., 2001).

Our recent results on the mechanism of Saethre-Chotzen syndrome, caused by heterozygous loss of function of *Twist1*, draw attention to the significance of tissue boundaries in the development of synostosis (Merrill et al., 2006). Individuals affected with Saethre-Chotzen have coronal synostosis, fusion of the frontal and parietal bones at the coronal suture. *Twist1* mutant mice also exhibit coronal synostosis (Carver et al., 2002; el Ghouzzi et al., 1997). In such mice and in cultured osteoblasts, *Twist1* can inhibit osteoblast differentiation by regulating the activity of *Runx2* (Bialek et al., 2004; Guenou et al., 2005; Yoshida et al., 2005). Connerney et al. have presented evidence that reduced dosage of Twist1 changes the proportion of Twist1 homo- and heterodimers within developing sutures and thereby regulates suture patency (Connerney et al., 2008; Connerney et al., 2006). We demonstrated that *Twist1* mutant mice have a deficiency in the neural crest-mesoderm boundary at the coronal suture (Merrill et al., 2006). The boundary normally lies between the mesoderm-derived cells of

Department of Biochemistry and Molecular Biology, Norris Cancer Hospital, University of Southern California Keck School of Medicine, 1441 Eastlake Avenue, Los Angeles, CA 90089-9176, USA.

*Author for correspondence (maxson@usc.edu)

Accepted 22 December 2008

the prospective suture and the neural-crest-derived osteogenic cells of the prospective frontal bone (Merrill et al., 2006; Yoshida et al., 2008). Thus the boundary not only demarcates neural crest and mesoderm, but also osteogenic and non-osteogenic sutural cells. In *Twist1* mutants, neural crest cells crossed the boundary into the mesoderm domain of the suture (Merrill et al., 2006).

We showed previously that the change in cell behavior at this boundary was associated with a reduction in the levels of the ephrin ligands, ephrin A2 (Efna2) and ephrin A4 (Efna4), as well as their receptor, EphA4. Moreover, we identified loss-of-function mutations in *EFNA4* in 3/77 patients (Merrill et al., 2006). Ephrins are membrane-bound ligands that interact with Eph receptors, a large family of receptor tyrosine kinases (Klein, 2004; Kullander and Klein, 2002; Wilkinson, 2001). Ephrin-Eph signaling is bidirectional, through both the receptor and the ligand. Engagement of Eph receptors by membrane-bound ephrin ligands induces dimerization and subsequent trans-phosphorylation of the receptors, leading to changes in the activity of downstream effectors, which include the mitogen-activated protein kinases ERK, c-Jun N-terminal kinase, Src family kinases and Ras/Rho family GTPases. Ephrin-Eph signaling regulates a variety of developmental processes including vascular and neuronal development and the establishment of developmental boundaries (Klein, 2004; Kullander and Klein, 2002; Martinez and Soriano, 2005; Palmer and Klein, 2003; Pasquale, 2005; Poliakov et al., 2004; Surawska et al., 2004).

Here we test for a causal connection between *Twist1*, ephrin A signaling and craniosynostosis; we also investigate cellular mechanisms controlled by ephrin A signaling in the developing skull vault. We demonstrate that loss of function of the *Efna4* receptor, *EphA4*, causes coronal synostosis in mice, definitively establishing the link between craniosynostosis and loss of ephrin A signaling suggested by our earlier human genetic findings (Merrill et al., 2006). We show further that *EphA4* interacts genetically with *Twist1* and acts as a *Twist1* effector in the control of the frontal-parietal boundary and in the regulation of the RTK indicator, P-Erk1/2 and the BMP pathway indicator, P-Smad1/5/8. Finally we use 1,1-dioctadecyl-3,3,3,3-tetramethylindocarbocyanine perchlorate (DiI) labeling to show that *Twist1* and *EphA4* control the guidance of migratory osteogenic cells to the leading edges of the growing frontal and parietal bones, and that these genes are required to exclude such osteogenic cells from the coronal suture. Our results suggest that migration of osteogenic cells is an important element in the patterned growth of calvarial bones, and that the mis-migration of such cells plays a crucial role in the development of craniosynostosis in *Twist1* and *EphA4* mutant mice.

MATERIALS AND METHODS

Mouse mutants and genotyping

The *EphA4* mutant mouse was a kind gift of Elena Pasquale; the *Efna2* mutant, of David Feldheim. Both mutant lines were maintained in a C57Bl/6 background. The *Twist1* (Chen and Behringer, 1995), *R26R* (Soriano, 1999), *Wnt1-cre* (Danielian et al., 1998) and *Mesp1-cre* (Saga et al., 1999) alleles have been described. We genotyped *EphA4*, *Efna2*, *Twist1*, *R26R*, *Wnt1-cre* and *Mesp1-cre* alleles by PCR as described (Chen and Behringer, 1995; Dottori et al., 1998; Feldheim et al., 2000; Jiang et al., 2002; Saga et al., 1999).

Histology, immunostaining and in situ hybridization

Heads of embryos were embedded in OCT medium (Histoprep, Fisher Scientific) before sectioning. Frozen sections were cut at 10 μm. Analysis of β-galactosidase activity of *Wnt1-Cre/R26R* and *Mesp1-Cre/R26R* reporter gene expression was carried out as described (Ishii et al., 2003). Immunostaining of frozen sections was largely carried out as previously reported (Ishii et al., 2003). Immunohistochemistry was performed using rabbit anti-Runx2 (Sigma), rabbit P-Erk1/2 (Cell Signaling), rabbit Erk1/2 (Cell Signaling) and rabbit anti-P-Smad1/5/8 (Cell Signaling) diluted in 1% BSA/PBS and incubated overnight at 4°C. Detection of primary antibody of anti-Runx2, anti-P-Erk1/2 and anti-Erk1/2 was performed by incubating goat anti-rabbit-HRP (Zymed, 1/250) for 1 hour at room temperature and visualizing with DAB substrate. Detection of anti-P-Smad1/5/8 was performed by incubating rhodamine-labeled goat anti-rabbit IgG (1:100) for 1 hour at room temperature followed by DAPI counterstaining and examination by epifluorescence microscopy. Non-radioactive section in situ hybridization using the tyramide signal amplification (TSA) method was performed as described (Adams, 1992; Paratore et al., 1999; Yang et al., 1999). Briefly, to analyze mRNA expression by TSA, DIG-labeled or FL-labeled riboprobes were allowed to hybridize with the section and were detected with anti-DIG or anti-FL antibodies conjugated to horseradish peroxidase (POD). Indirect TSA fluorescence system (TSA-biotin/avidin-FITC) was used to detect the POD-conjugated antibody (Perkin Elmer). RNA probes were generated as reported: *EphA4* (Nieto et al., 1992), *Twist1* (Rice et al., 2000).

Whole-mount skull Alizarin Red S staining

Skulls from 21-day-old postnatal mice were stained for bone with 2% Alizarin Red S in 1% KOH for 1 to 2 days. The specimens were then cleared and stored in 100% glycerol.

Whole-mount alkaline phosphatase (ALP) staining

Whole-mount staining for alkaline phosphatase was carried out as described (Ishii et al., 2003). Embryonic day 13.5 (E13.5) embryo heads were fixed in 4% paraformaldehyde in PBS, and were bisected midsagitally after fixation. Presumptive calvarial bones were stained with NBT and BCIP (Roche).

Exo utero DiI labeling of migratory osteogenic precursor cells

Details of the exo utero manipulation have been described (Muneoka et al., 1986; Serbedzija et al., 1992). Briefly, E13.5 embryos with embryonic membranes were carefully exposed by incising the uterine wall. Two embryos from each side of the uterine horns were designated as the experimental group, and all others were removed. DiI (Molecular Probes, 1:10 dilution from 0.5% stock solution) was injected into the area of the calvarial bone rudiments under a dissecting microscope with a microelectrode (tip diameter, 20 μm) attached to a mouth pipette (Yoshida, 2005). After injection, the embryos were returned to the peritoneal cavity of dams and allowed to continue development exo utero. After 2-3 days of additional development, the embryos were removed and examined by epifluorescence microscopy. The survival rate of the embryos after DiI injection was greater than 70%.

RESULTS

Loss of EphA4 function causes coronal synostosis and defective formation of the neural crest-mesoderm boundary at the coronal suture

We first examined the morphology of coronal sutures in individual $EphA4^{-/-}$ and $Efna2^{-/-}$ mutant mice (an *Efna4* mutant was not available). In addition, because ephrins can function redundantly with their receptors (Wang et al., 1999), we assessed compound $EphA4^{-/-}; Efna2^{+/-}$ mutant mice. Alizarin-Red staining of skulls of $EphA4^{-/-}$ mice at P21 revealed that the coronal sutures were partially fused, a phenotype that closely resembles that of $Twist1^{+/-}$ mice (Fig. 1). $Efna2^{-/-}$ mutants exhibited normal coronal suture development. $EphA4^{-/-}; Efna2^{+/-}$ double mutant skulls had no significant increase in the severity of the synostosis phenotype over $EphA4^{-/-}$ mutants (Fig. 1; data not shown), indicating that *EphA4* plays a more prominent role than *Efna2* in coronal synostosis, at least in the mouse. We therefore concentrated on *EphA4* mutants in further efforts to understand the relationship between *Twist1*, ephrin signaling and craniosynostosis.

We examined the activity of alkaline phosphatase (ALP), an early osteoblast marker, in $EphA4^{-/-}$ embryos at E14.5 when a loss of integrity of the boundary between ALP and non ALP-expressing

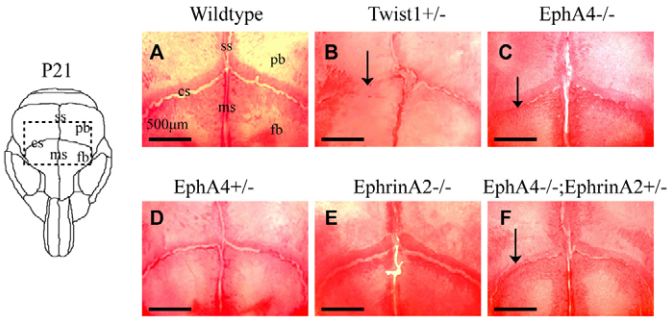

Fig. 1. Fusion of coronal sutures in *EphA4* mutant mice. Skulls of animals at P21 were stained with Alizarin Red S and photographed. The diagram (left) shows the area depicted in the photographs. Note open coronal sutures in control (**A**), *EphA4*$^{+/-}$ (**D**) and *Efna2*$^{-/-}$ (**E**); note partially fused sutures in *Twist1*$^{+/-}$ (**B**) and *EphA4*$^{-/-}$ (**C**), and little or no influence of *Efna2* genotype on suture fusion in *EphA4*$^{-/-}$ mutant (**F**). cs, coronal suture; fb, frontal bone; ms, metopic suture; pb, parietal bone; ss, sagittal suture.

cells is first apparent in *Twist1* mutants (Merrill et al., 2006) (Fig. 2). In wild-type embryos, the prospective coronal suture is evident as a layer of non-ALP-expressing cells located between the prospective frontal and parietal bones. In *EphA4*$^{-/-}$ mutants this layer exhibited a disorganized appearance and was filled with ALP-expressing cells, as is the case in *Twist1*$^{+/-}$ mutants (Fig. 2) (Merrill et al., 2006). In addition, the expression domain of ALP was substantially broader in *EphA4*$^{-/-}$ mutants, similar to a phenotype observed in *Twist1* mutants.

In parallel, we assessed the status of the neural crest-mesoderm boundary by means of the *Wnt1-Cre; R26R* neural-crest-lineage marking system (Jiang et al., 2002) (Fig. 2). We carried out intercrosses between *EphA4* mutants and embryos carrying *Wnt1-Cre* and *R26R* and examined embryos at a series of developmental stages. In *EphA4*$^{-/-}$ mutants, *lacZ*-positive cells were evident outside the neural crest domain. This phenotype was first detectable at E14.5 and became more severe at E16.5. We did not detect a boundary defect in heterozygous mutants. These results suggest that reduced *EphA4* function results in a set of phenotypes in the coronal suture that resemble those of *Twist1* mutants.

EphA4 is a downstream effector of *Twist1* in the coronal suture

We sought to determine whether levels of *EphA4* transcripts in the developing calvarial bones and sutures are regulated by *Twist1* (Fig. 3). *EphA4* mRNA was localized in the periosteal layers above and below the developing frontal and parietal bones. It was also expressed in a layer of cells outside (ectocranial to) the bone layer, and broadly within the suture mesenchyme. In *Twist1*$^{+/-}$ mutants, *EphA4* expression was reduced substantially in the ectocranial and periosteal layers, consistent with our previous finding that *Twist1* controls the levels of EphA4 protein expression in calvarial tissues. *Twist1* expression was not changed in *EphA4*$^{-/-}$ mutants.

If *EphA4* is an effector of *Twist1*, then combination *Twist1*$^{+/-}$; *EphA4*$^{+/-}$ heterozygotes should exhibit phenotypes of greater severity than individual heterozygous mutants. We crossed *Twist1*$^{+/-}$ heterozygous mice with *EphA4* mutant mice and examined skulls at E13.5, E14.5 and P21 (Fig. 4; Table 1). The penetrance of craniosynostosis as assessed at P21 increased from

Table 1. Influence of genotype on the penetrance of craniosynostosis

Genotype	Number of mice with fused coronal suture
Wild type	0/20
EphA4$^{+/-}$	0/16
Efna2$^{-/-}$	0/9
EphA4$^{+/-}$; *Efna2*$^{+/-}$	0/14
EphA4$^{-/-}$	8/20*
EphA4$^{-/-}$; *Efna2*$^{+/-}$	8/17*
Twist1$^{+/-}$	19/26
Twist1$^{+/-}$; *EphA4*$^{+/-}$	31/33

Fusion of the coronal suture was assessed at P21 in Alizarin Red S-stained whole-mount skulls.
*No significant difference in penetrance was observed between *EphA4*$^{-/-}$ and *EphA4*$^{-/-}$; *EphA2*$^{+/-}$ (P>0.05).

73 to 94% in *Twist1*$^{+/-}$; *EphA4*$^{+/-}$ compound mutants (n=33) compared with Twist1$^{+/-}$ mutants (n=26); also, a larger portion of the suture was fused (50 vs 25%; P<0.005) in the compound mutants.

Whole-mount ALP stains of embryonic heads showed that whereas at E12.5 there was no difference in the ALP expression domain between mutants and control embryos (data not shown), by E13.5 there was a substantial change (Fig. 4). In combination heterozygotes, the ALP domain expanded into the coronal suture (Fig. 4A-C). Expression of the osteoblast markers ALP and Runx2 in sections through the coronal suture revealed a significant increase in the number of osteogenic cells within the sutures of compound heterozygotes compared with individual heterozygotes. Mutants also had ectopic Runx2-positive cells in the non-osteogenic layer ectocranial to the osteogenic layer (Fig. 4D-F). These data suggest that *Twist1* and *EphA4* cooperatively control the number and distribution of osteogenic cells in the coronal suture and ectocranial mesenchyme.

Twist1 and *EphA4* cooperatively control P-Erk1/2 and P-Smad1/5/8 activity in the developing frontal and parietal bones

As part of an effort to understand the molecular basis of the suture defects, we examined the expression of the RTK effector, P-Erk1/2 (Fig. 5), and the BMP effector, P-Smad1/5/8 (Fig. 6). *Twist1* and Eph-ephrin are known to function through the RTK pathway (Guenou et al., 2005; Pratt and Kinch, 2002; Vindis et al., 2003). FGF/FGFR signaling has a well-documented role in craniosynostosis and normal suture development (Deng et al., 1996; Johnson et al., 2000; Marie et al., 2005; Rice et al., 2000; Yamaguchi and Rossant, 1995), and *Twist1* has been shown to control levels of FGFR expression and P-Erk1/2 activity in sutures of late embryonic and postnatal mice (Connerney et al., 2008; Rice et al., 2000). Finally, the BMP pathway is known to be involved in the specification and differentiation of calvarial osteogenic cells (Kim et al., 1998; Ryoo et al., 2006); forced expression of the BMP antagonist *noggin* can prevent fusion of the sagittal suture (Warren et al., 2003).

Immunostaining of sections of E14.5 embryos showed that P-Erk1/2 was expressed in the ectocranial non-osteogenic cell layer as well as in the underlying osteogenic layer (Fig. 5). The number of P-Erk1/2-expressing cells decreased progressively in both layers as the dosages of *Twist1* and *EphA4* were reduced. Total Erk was unaffected in *Twist1*$^{+/-}$; *EphA4*$^{+/-}$ mutants, demonstrating that *Twist1* and *EphA4* specifically regulate the distribution of cells expressing phosphorylated Erk1/2.

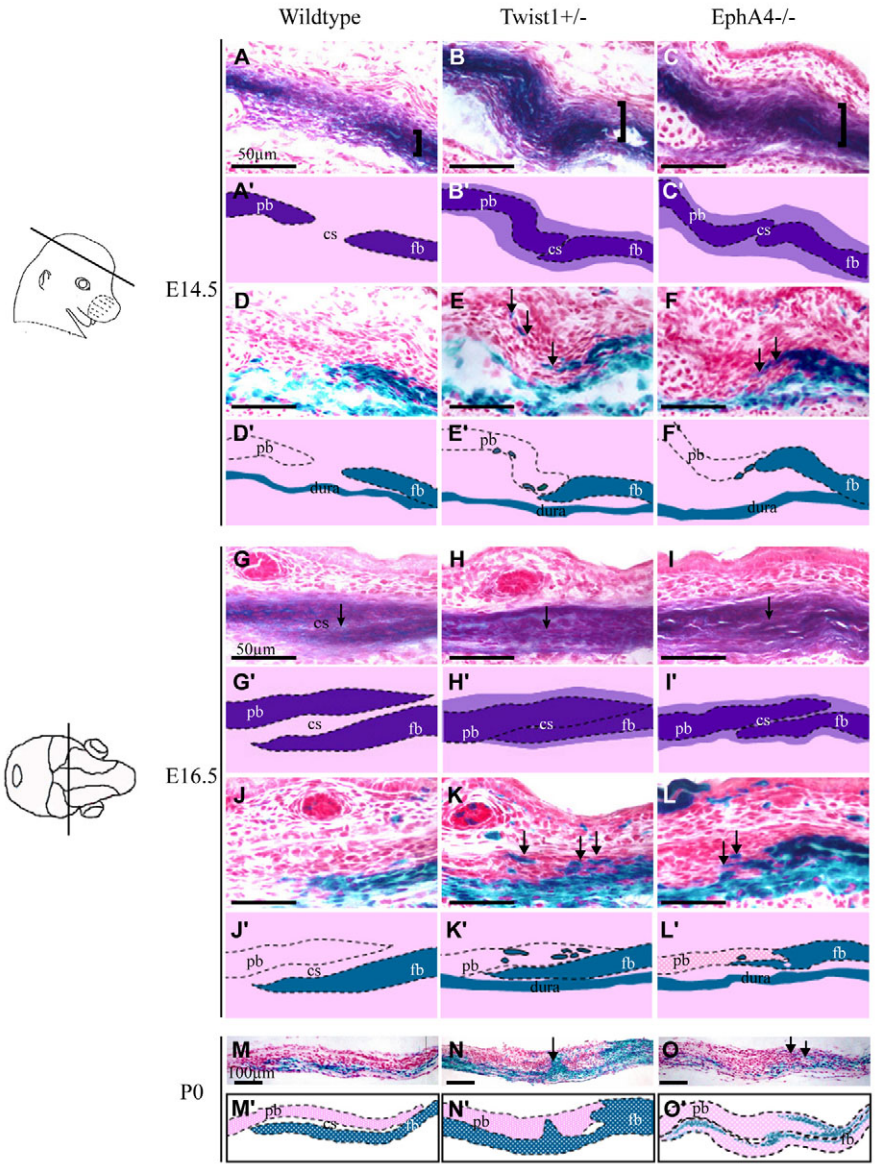

Fig. 2. Increased number of alkaline phosphatase-expressing cells and defect in the neural crest-mesoderm boundary in coronal sutures of *EphA4*$^{-/-}$ embryos. Heads of wild-type *Wnt1-Cre; R26R*, *Twist1*$^{+/-}$*; Wnt1-Cre; R26R*, and *EphA4*$^{-/-}$*; Wnt1-Cre; R26R* embryos at E14.5, E16.5 were sectioned in the plane indicated and alternate sections were stained either for alkaline phosphatase (**A-C** and **G-I**) or *lacZ* expression (**D-F** and **J-L**). Pups at P0 were examined only for *lacZ* expression (**M-O**). Schematics depicting key results are shown below each image (**A′-O′**). Note widening of ALP domain (A-C, brackets) and expansion of ALP expression into suture (G-I, arrows). Also note *lacZ*-positive (neural crest) cells located ectopically in prospective coronal suture and parietal bone (D-F,J-L,M-O, arrows). cs, coronal suture; fb, frontal bone; pb, parietal bone.

The distribution of P-Smad1/5/8-expressing cells was also strongly influenced by *Twist1* and *EphA4* (Fig. 6). Control embryos expressed P-Smad1/5/8 at a high level in the osteogenic fronts of the growing frontal and parietal bones (Fig. 6A,B). Lower levels were evident in more mature osteoblasts, distal to the leading edges. Thus, at E14.5, the highest levels of P-Smad1/5/8 activity were associated with the progenitor cells of the osteogenic fronts and lower levels with the differentiated cells of the developing bone. There was a clear boundary between domains of high and low P-Smad1/5/8 expression in the osteogenic fronts and suture. In both *Twist1* and *EphA4* mutants, the number of P-Smad1/5/8-expressing cells was reduced significantly in the osteogenic fronts, and the boundary between these cells and the prospective sutural cells was blurred (Fig. 6E-L). Punctate staining of P-Smad1/5/8 was evident throughout the suture. Combination mutants exhibited an even more dramatic reduction in the number of P-Smad1/5/8-positive cells in the suture (Fig. 6M,N). These data suggest that *Twist1* and *EphA4* together control the number and distribution of P-smad1/5/8-positive cells in the coronal suture. Further, the reduction in the number of P-Smad1/5/8-expressing cells in the suture is consistent with our finding that high levels of P-Smad1/5/8 expression are associated with undifferentiated progenitor cells in the osteogenic fronts, and lower levels with differentiating osteogenic cells within developing bone.

Twist1 and *EphA4* are required for the proper partitioning of migratory osteogenic cells between osteogenic and non-osteogenic territories in the coronal suture

Wnt1-Cre/R26R analysis of *Twist1*$^{+/-}$*; EphA4*$^{+/-}$ embryos at E16.5 (Fig. 7), as well as E14.5 and P0 (not shown), demonstrated that relative to wild type or individual heterozygotes, a larger number of neural crest cells crossed into the undifferentiated mesoderm (Fig. 7A-C′; see also Fig. 2). Complementary results came from an assessment of the mesoderm lineage by means of the pan mesoderm marker, *Mesp1-Cre/R26R* (Fig. 7D-F′). In control embryos, *Mesp1-Cre*-directed *lacZ* expression was the inverse of the *Wnt1-Cre lacZ* domain: *lacZ*-positive cells were evident in the parietal bone, and in the layer of cells ectocranial to the parietal and frontal bones. There was strong labeling of the non-osteogenic cells interposed between

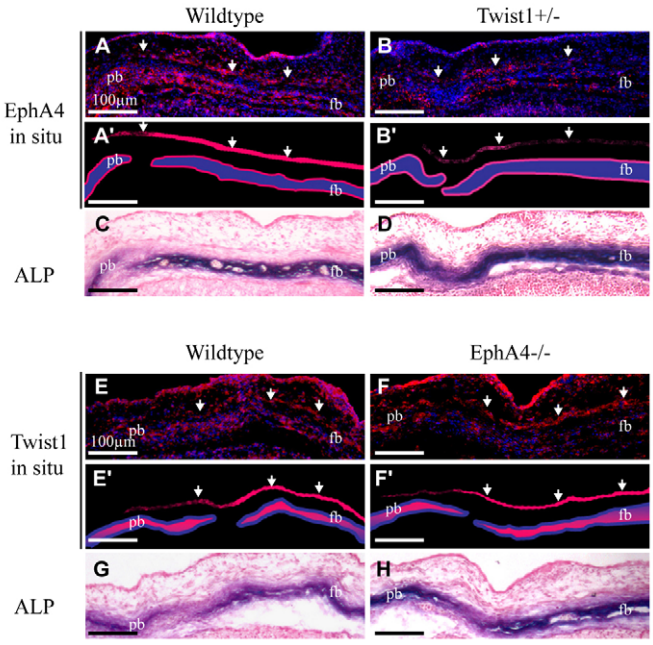

Fig. 3. Altered expression of *EphA4* mRNA in *Twist1* mutant suture. Probes against *EphA4* (**A-B'**) or *Twist1* (**E-F'**) mRNA were incubated with sections of wild-type, *Twist1*$^{+/-}$ or *EphA4*$^{-/-}$ embryos at E14.5. Alternate sections were stained for ALP activity (**C**,**D**,**G**,**H**). Note co-expression of *EphA4* and *Twist1* in ectocranial mesenchyme (arrows). Also note reduced expression of *EphA4* in *Twist1*$^{+/-}$ mutant but unchanged expression of *Twist1* in *EphA4*$^{-/-}$ mutant. Plane of section was as in Fig. 2. fb, frontal bone; pb, parietal bone.

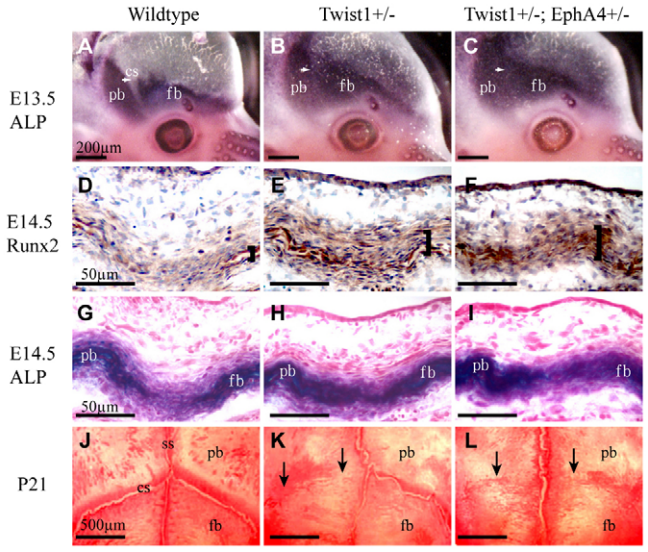

Fig. 4. Genetic interaction between *Twist1* and *EphA4*. Heads of wild-type, *Twist1*$^{+/-}$ and *Twist1*$^{+/-}$; *EphA4*$^{+/-}$ embryos were examined for the expression of ALP and the osteoblast determinant, *Runx2*. ALP was assessed by histochemistry, Runx2 by immunostaining. Skulls of P21 animals were stained with Alizarin Red (**J-L**). Note progressive loss of ALP-free zone of coronal suture with reduction of *Twist1* and *EphA4* dosage (**A-C**). Also note increased staining of Runx2 and ALP in sections of heads at E14.5 (**D-I**) and increased coronal suture fusion in skulls of P21 mice (J-L). cs, coronal suture; fb, frontal bone; pb, parietal bone; ss, sagittal suture.

the frontal and parietal bones, i.e. the mesenchyme of the coronal suture. These results are consistent with the recent report of Yoshida et al. (Yoshida et al., 2008). In embryos with the *Twist1*$^{+/-}$; *EphA4*$^{+/-}$ genotype, a substantial number of *lacZ*-positive cells were ectopically located in the neural crest territory. Thus cells derived from mesoderm, as well as neural crest, failed to respect the neural crest-mesoderm boundary between the frontal and parietal bones.

These data raised the possibility that a contributing cause of synostosis is the replacement or dilution of non-osteogenic sutural cells with osteogenic cells from adjacent territories. To test this hypothesis further, we used DiI labeling of embryos, exo utero (Yoshida, 2005; Yoshida et al., 2008). This allowed us to examine directly the behavior of populations of migratory osteogenic cells that contribute to the frontal and parietal bones. At E12.5, the frontal and parietal bone rudiments consist of patches of osteogenic precursor cells located in the supraorbital ridge. The frontal bone rudiment is anterior to the eye, the parietal bone rudiment is posterior. Between the rudiments is the prospective coronal suture, in later stages identifiable by the absence of ALP-expressing osteogenic cells. The prospective frontal and parietal osteogenic cells can be labeled by injecting DiI into the area of the rudiments (supraorbital ridge) at E13.5 (Yoshida, 2005; Yoshida et al., 2008) (P.G.R., N.L.W. and R.E.M., unpublished observations). During subsequent development of the injected embryos, exo utero, labeled cells migrate apically, adding to the leading edge of the frontal and parietal bones.

We asked whether such migratory osteogenic cells exhibit abnormal behavior in *Twist1-EphA4* mutants. We injected DiI into E13.5 *Twist1*$^{+/-}$; *EphA4*$^{+/-}$ embryos and allowed them to develop exo utero. We then examined the embryos at E16.5 by epifluorescence microscopy. As is evident in Fig. 8, labeled cells were excluded from the area of the prospective suture in wild-type embryos. However, such cells were present in substantial numbers in the sutural space of *Twist1*$^{+/-}$; *EphA4*$^{+/-}$ mutant embryos. In multiple repetitions of this experiment, in which DiI was injected into the frontal bone rudiment as well as the parietal bone rudiment, we obtained closely similar results (Table 2). Thus, *Twist1* and *EphA4* controlled the distribution of migratory osteogenic precursor cells between the non-osteogenic coronal suture and the prospective frontal and parietal bones. We also examined the distribution of migratory osteogenic precursor cells one day earlier when they are in the process of migration. In control embryos at E15.5, DiI-labeled cells were found largely in the ectocranial, EphA4-expressing layer (Fig. 8O-Q). In *EphA4-Twist1* mutants, by striking contrast, labeled cells were located diffusely within and adjacent to the osteogenic layer (Fig. 8R-T). Thus *Twist1* and *EphA4* determined the partitioning of osteogenic precursor cells between the non-osteogenic ectocranial layer and the ALP-expressing prospective bone. Together these results suggest that *Twist1* and *EphA4* function in the partitioning of migratory osteogenic cells between osteogenic and non-osteogenic territories in the coronal suture.

DISCUSSION

The proper guidance of migratory cells is crucial for a large variety of developmental processes. Here we provide evidence that ephrin-Eph signaling, under the control of *Twist1*, is required to exclude migratory osteogenic cells from normally non-osteogenic territories in the developing skull vault, including the coronal suture. We show in addition that *EphA4* is a *Twist1* effector, and that loss of *EphA* signaling is causally linked to craniosynostosis, as suggested by our

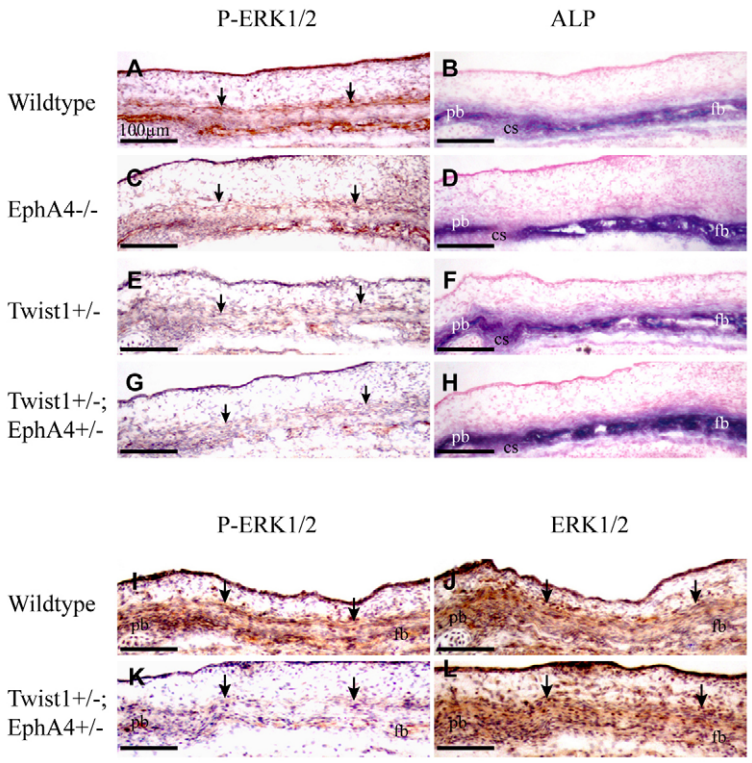

Fig. 5. Co-regulation of Erk1/2 phosphorylation in developing coronal suture by *Twist1* and *EphA4*. (**A-H**) Heads of E14.5 embryos with the indicated genotypes were sectioned as in Fig. 2 and stained either for P-Erk1/2 or ALP. (**I-L**) Sections were stained for P-Erk1/2 (I,K) or total Erk (J,L). Note progressive reduction in P-Erk1/2 staining in ectocranial layer (arrows) as dosage of *Twist1* and *EphA4* are reduced. Note also that total Erk1/2 is unaffected in *Twist1*$^{+/-}$; *EphA4*$^{+/-}$ embryos whereas P-Erk1/2 is substantially reduced. Thus *Twist1* and *EphA4* regulate Erk1/2 phosphorylation specifically. cs, coronal suture; fb, frontal bone; pb, parietal bone.

earlier identification of loss-of-function mutations in *EFNA4* in humans with non-syndromic coronal synostosis (Merrill et al., 2006).

Both the penetrance and the severity of craniosynostosis increased significantly in *Twist1*$^{+/-}$; *EphA4*$^{+/-}$ mutants compared with individual heterozygotes, demonstrating that *Twist1* and *EphA4* cooperate in the control of coronal suture development. That *EphA4* was downregulated in *Twist1* mutant sutures, whereas *Twist1* expression was not altered in *EphA4* mutants suggests that *Twist1* is upstream of *EphA4*. An *Efna2* mutant allele did not significantly enhance calvarial phenotypes caused by mutations in either *Twist1* or *EphA4*. *Efna2* is expressed in a pattern that overlaps substantially with *Efna4* (Merrill et al., 2006); thus *Efna2* and *Efna4* may function redundantly. However, in our earlier screen of patients with non-syndromic craniosynostosis we did not detect mutations in *Efna2* (Merrill et al., 2006). A definitive test of the roles of *Efna2* and *Efna4* in suture development will have to await an *Efna4* knockout mouse.

Table 2. Location of labeled cells following DiI injection into frontal or parietal bone rudiments

Experiment	Genotype	Rudiment injected	Location of labeled cells after migration
1	*EphA4*$^{+/-}$	p	p
2	Wild type	p	p
2	*Twist1*$^{+/-}$; *EphA4*$^{+/-}$	p	p, cs
3	*Twist1*$^{+/-}$	f, p	f, p, cs
3	Wild type	f, p	f, p
4	*Twist1*$^{+/-}$; *EphA4*$^{+/-}$	f, p	f, p, cs
4	Wild type	f, p	f, p
5	*Twist1*$^{+/-}$; *EphA4*$^{+/-}$	f, p	f, p, cs
6	*Twist1*$^{+/-}$	f, p	f, p, cs
6	*EphA4*$^{+/-}$	f, p	f, p
6	*Twist1*$^{+/-}$; *EphA4*$^{-/-}$	f, p	f, p, cs
7	*Twist1*$^{+/-}$; *EphA4*$^{-/-}$	f, p	f, p, cs

f, frontal bone; p, parietal bone; cs, coronal suture.

The expansion of osteogenic marker gene expression into the mesenchyme of the coronal suture is associated with a reduction in P-Erk1/2 activity in the non-osteogenic, ephrin A-expressing layer outside the osteogenic layer. Total Erk activity is not affected, demonstrating that *Twist1* and *EphA4* control P-Erk1/2 signaling specifically. It is interesting that this change in P-Erk1/2 is in the cell layer in which osteogenic precursor cells migrate, and from which migratory cells are lost in *Twist1-EphA4* combination mutants. Thus the phosphorylation status of Erk, which is known to be regulated by ephrin-Eph signaling (Elowe et al., 2001; Miao et al., 2001; Pasquale, 2008; Poliakov et al., 2004; Pratt and Kinch, 2002; Schmucker and Zipursky, 2001), may be related to the migratory properties of osteogenic precursor cells and to their association with this cell layer.

We note that our results on P-Erk1/2 levels are in apparent contrast with two recent findings. Yin et al. (Yin et al., 2008) found that an increase in P-Erk1/2 activity is associated with craniosynostosis in the Pro253Arg mutant of Fgfr2, which models Apert craniosynostosis; Connerney et al. (Connerney et al., 2008) showed that P-Erk1/2 is upregulated in sutures of Twist1 mutant mice. These results differ from ours in two important respects. First, both studies analyzed embryos at E16.5 or older, after the mis-migration/mixing events we document here have occurred. Second, both examined P-Erk1/2 activity at sites other than the ectocranial, EphA4-expressing layer. Yin et al. (Yin et al., 2008) in bone marrow cells and Connerney et al. (Connerney et al., 2008) in osteogenic fronts. These results, taken together with our findings, suggest that P-Erk signaling functions in two distinct processes, one at E15.5 or earlier, involving the partitioning of osteogenic cells between the EphA4-expressing layer and the osteogenic layer, the other at E16.5 or later involving the differentiation of osteogenic cells in the osteogenic layer or in the suture. The earlier process is positively regulated by *Twist1*, the later process negatively regulated.

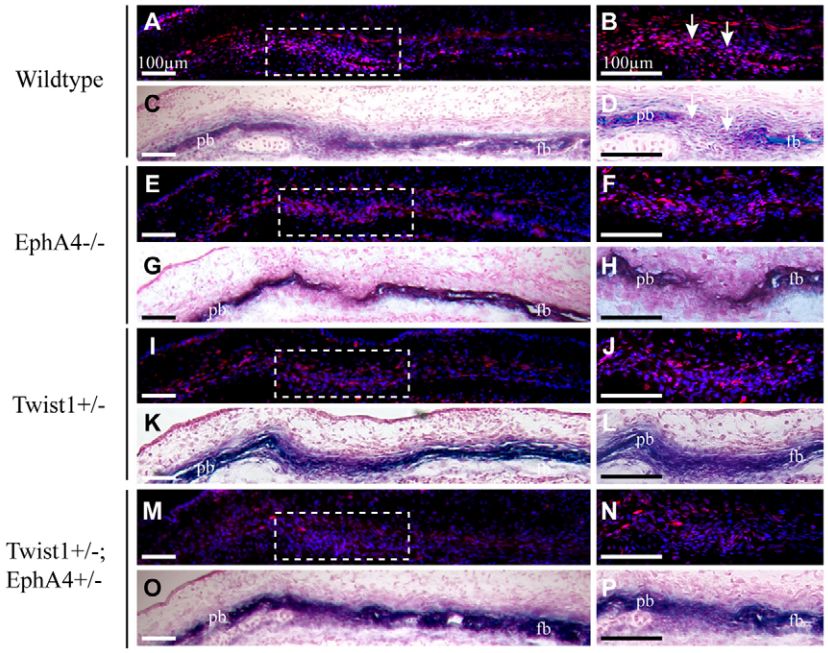

Fig. 6. Altered distribution of P-Smad1/5/8-expressing cells in coronal sutures of *Twist1* and *EphA4* individual and combination mutant embryos. Heads of E14.5 embryos were sectioned as in Fig. 2 and stained for P-Smad1/5/8 activity. Alternate sections were stained for ALP. Right panels show enlargements of dashed squares in left panels. Note concentration of stained nuclei in osteogenic fronts of wild-type embryos (**A-D**). In mutant embryos, note scattered stained nuclei and loss of concentration of stained nuclei in osteogenic fronts (**E-P**). fb, frontal bone; pb, parietal bone.

Also associated with the expansion of osteogenic marker gene expression into sutural mesenchyme in individual and combination *Twist1* and *EphA4* mutants is a broadening of the distribution of P-Smad1/5/8-expressing cells and a reduction in their number. That Smad1/5/8 signaling is apparently reduced in craniosynostotic sutures may seem paradoxical given the general finding that Bmp signaling promotes osteogenesis. However, we note that in wild-type sutures, high levels of P-Smad1/5/8 are found in osteogenic fronts, which contain proliferative, ALP-positive cells, and lower levels are found in differentiating osteoblasts within the developing bone. Thus while the Bmp pathway has a well-documented positive role in osteogenesis, the transition from proliferative osteogenic cells of the osteogenic front to more differentiated osteoblasts in the mineralizing bone may actually entail a reduction in Bmp signaling. We note that two studies have reported increases in P-smad1/5/8 levels or Bmp activity in craniosynostotic sutures (Warren et al., 2003; Connerney et al., 2008). However, both focused on late-embryonic or postnatal stages, and in the case of Warren et al. (Warren et al., 2003), on a sagittal suture. Thus, as with P-Erk1/2 signaling, it is likely that these studies concern processes distinct from the boundary and migration defects we document here.

Wnt1-Cre/R26R and *Mesp1-Cre/R26R* markers provide complementary results demonstrating a defect in the neural crest mesoderm boundary at the coronal sutures of *EphA4* and *Twist1-EphA4* mutants. On the neural crest side, Wnt1-Cre-labeled cells are fated to become osteogenic cells of the frontal bone. On the mesoderm side, Mesp1-Cre-labeled cells are fated to become either sutural (non-osteogenic) cells or parietal bone osteogenic cells, or cells of the ectocranial layer. It is interesting that neither *EphA4* nor any of the ephrin ligands we surveyed exhibit restricted expression at the neural crest-mesoderm boundary (Merrill et al., 2006) (A. Merrill and R.E.M., unpublished), suggesting that ephrin signaling controls boundary behavior not by regulating cell interactions at the immediate boundary, but by controlling the guidance or migratory behavior of osteogenic cells as they move apically from the frontal and parietal bone rudiments in the supraorbital ridge to the leading

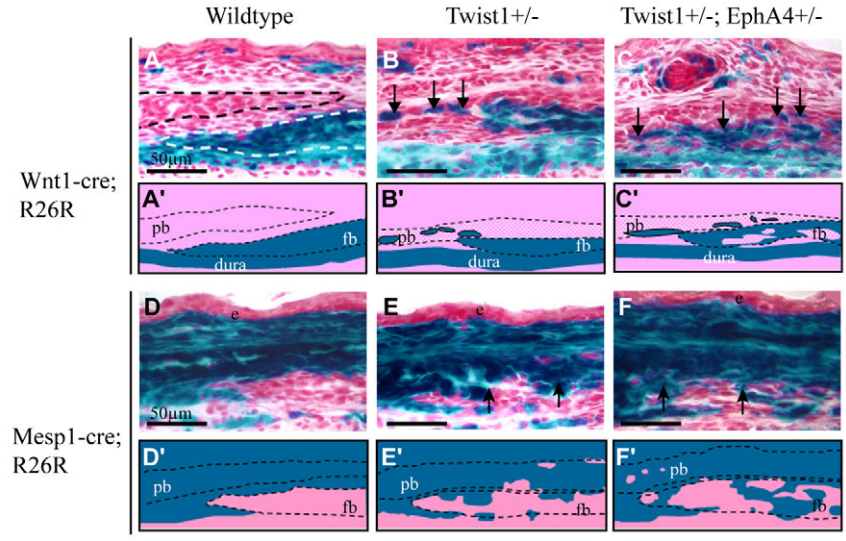

Fig. 7. Cooperative control of neural crest-mesoderm boundary at coronal suture by *Twist1* and *EphA4*. Either the neural crest marker *Wnt1-Cre; R26R* or the mesoderm marker *Mesp1-Cre; R26R* was crossed into mice with the indicated genotypes. Heads of E16.5 embryos were sectioned as in Fig. 2 and stained for *lacZ*. Schematics depicting key results are shown below each image. Note sharp mesoderm-neural crest boundary in wild-type embryo (**A**,**A′**,**D**,**D′**). Note both neural crest-derived cells and mesoderm-derived cells crossing boundary in mutant embryos. Also note increased severity of boundary defect in *Twist1*$^{+/-}$; *EphA4*$^{+/-}$ embryo (**C**,**C′**,**F**,**F′**) compared with *Twist1*$^{+/-}$ embryo (**B**,**B′**,**E**,**E′**).

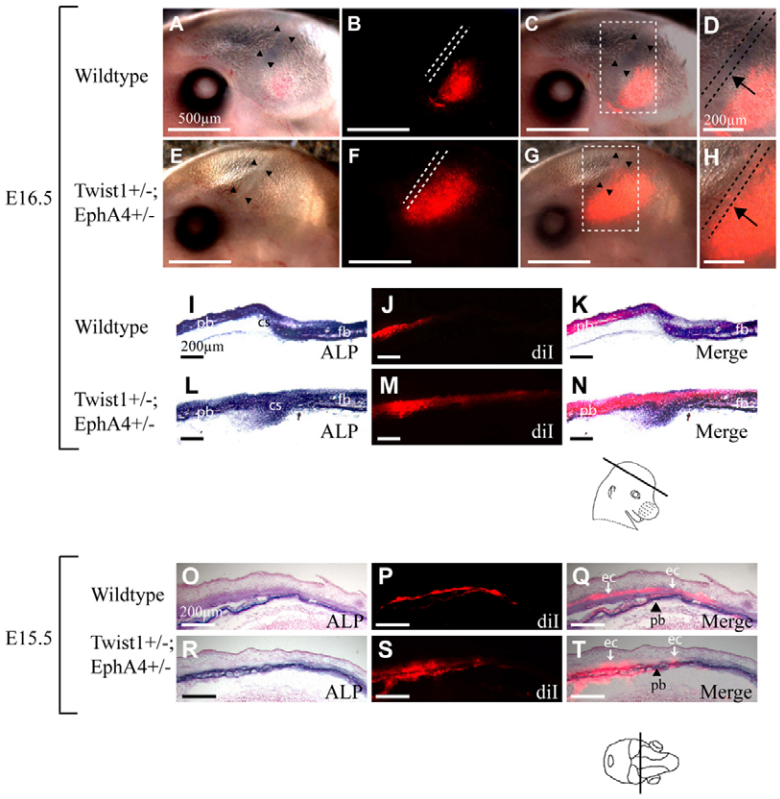

Fig. 8. Mis-migration of osteogenic precursor cells in *Twist1*$^{+/-}$; *EphA4*$^{+/-}$ mutant embryos. We injected DiI into parietal bone rudiments of E13.5 wild-type (**A-D**,**I-K**,**O-Q**) and mutant (**E-H**,**L-N**,**R-T**) embryos, in vivo. Embryos were allowed to develop exo utero to E16.5 (A-N) or E15.5 (O-T), when they were examined for the distribution of DiI by epifluorescence microscopy. Sections shown in I,K,L,N,O,Q,R and T were also stained for ALP activity. E16.5 (A-N): embryos shown in whole mount in A-H were sectioned; images of the sections are shown in I-N. (A,E) Brightfield images of whole mounts. Note location of coronal sutures (arrowheads). (B,F) Epifluorescence images, with dotted lines showing location of sutures. (C,G) Merged brightfield and epifluorescence images. Area within dashed square is magnified in D,H. Labeled osteogenic precursor cells migrate apically (B-D) and insert into the growing bone (J,K). Note DiI-labeled cells are excluded from coronal sutures of wild-type (B,D, dotted lines) but not mutant embryos (G,H arrows). This is also clearly evident in sections: compare J,K with M,N. E15.5 (O-T): images are from coronal sections of E15.5 embryos (plane of section indicated). (O,R) Brightfield images stained for ALP; (P,S) epifluorescence images; (Q,T) combined brightfield and epifluorescence images. Note that in wild-type embryos, labeled cells are located largely in layer flanking (ectocranial to) the osteogenic layer (arrows, 'ec'). In mutant embryos, labeled cells are located diffusely in and around osteogenic layer of parietal bone (arrowheads, 'pb'). Closely similar results were obtained in more than ten injected wild-type embryos and three injected mutant embryos.

edges of the developing bone. We investigated this hypothesis by means of DiI labeling of embryos in vivo, followed by exo utero development of injected embryos. Iseki and colleagues used this technique to demonstrate that migratory cells contribute to the growing calvarial bones (Yoshida, 2005; Yoshida et al., 2008). We used this approach because of the lack of a satisfactory means of labeling and culturing calvarial rudiments in vitro in a way that mimics normal apical expansion of the frontal and parietal bones. This labeling technique enables us follow cells injected at E13.5 for periods of up to five days with no significant dilution of DiI. Moreover, development of injected embryos is normal.

The recent work of Yoshida et al. (Yoshida et al., 2008), together with our results (Fig. 8), demonstrates that DiI injected into the frontal or parietal bone rudiments labels osteogenic precursor cells. Our finding that cells labeled by injection of DiI into the parietal bone rudiment are present in the coronal suture of mutant mice strongly suggests that these are cells that would normally contribute to the parietal bone. Thus, from *Wnt1-Cre* and *Mesp1-Cre* lineage tracing, together with DiI labeling, we conclude that in *Twist1-EphA4* mutant mice, osteogenic cells of neural crest and mesoderm origin cross a boundary between the osteogenic territories of the frontal and parietal bones and enter the coronal suture. We conclude further that the normal function of ephrin-Eph signaling is to target cells to appropriate sites at the coronal leading edge of the bone and ensure that they do not enter the coronal suture. How ephrin-Eph signaling achieves this remains unclear, although such signaling is known to guide cells by means of repulsive and attractive interactions (Arvanitis and Davy, 2008; Egea and Klein, 2007; Klein, 2004; Santiago and Erickson, 2002).

Twist1 mutant mice exhibit synostosis of the lambdoid suture as well as the coronal (H. Yen and R.E.M., unpublished observations). The lambdoid suture does not coincide with a major lineage boundary like the coronal, raising the question of the extent to which boundary defects are involved in lambdoid synostosis. Our Cre labeling and DiI labeling results suggest that it is not the neural crest-mesoderm boundary per se that is important in the development of coronal synostosis, but rather a defect in a boundary between osteogenic and non-osteogenic compartments. We suggest that such a mechanism may apply generally to the lambdoid and other sutures.

What is the role of mistargeting of osteogenic cells in the development of synostosis? That reduced dosage of the osteoblast determinant *Runx2* can rescue the *Twist1* synostosis phenotype (Bialek et al., 2004) suggests that inappropriate differentiation of osteogenic cells is part of the mechanism underlying synostosis in *Twist1* mutants. Our present data show that in control embryos migratory osteogenic cells migrate apically along the ectocranial layer, ultimately reaching the leading edge of the bone. In mutant embryos, migratory osteogenic cells are excluded from the ectocranial layer, moving into the osteogenic layer and the prospective suture. Consequences of this include the broadening of ALP activity in the osteogenic layer, the presence of ALP-positive cells in the coronal at E14.5, and the ultimate formation of bone within the suture. We suggest that two mechanisms – aberrant migration and a change in osteogenic cell differentiation requiring Runx2 – work in sequence to produce synostosis. We propose that osteogenic cells from the frontal and parietal territories invade the coronal suture and signal normally non-osteogenic sutural cells to assume an osteogenic identity, thus producing synostosis.

Finally we note that our findings are consistent with the recent results of Yoshida et al. (Yoshida et al., 2008) in supporting the view that cell migration is a significant morphogenetic force in the patterned growth of the skull vault. Lana-Elola et al. (Lana-Elola et al., 2007) showed that only a small number of cells of the mesenchyme of the sagittal suture assume an osteogenic identity and are incorporated into the advancing parietal bone (Lana-Elola et al.,

2007). However, inhibition of DNA synthesis slowed bone growth significantly, leading these authors to propose that proliferation of cells of the osteogenic fronts rather than recruitment of prepositioned mesenchyme is important for bone growth. Our results, together with those of Yoshida et al. (Yoshida et al., 2008) suggest that migration of osteoprogenitor cells from an area at the base of the growing rudiment also makes a major contribution to the apical expansion of calvarial bones. More precise identification of these progenitor cell populations, as well as an understanding of the processes that guide their migration and differentiation will illuminate the mechanisms that underlie the patterned growth of the skull as well as the pathophysiology of craniosynostosis.

We thank Drs Mamoru Ishii, Hai-Yun Yen, Amy E. Merrill, Inna Gitelman and Christopher Schafer for helpful discussions. This work was supported by NIH grants DE12941 and DE12450 (R.E.M.), a grant from the California Institute of Regenerative Medicine (T1-00004), and grant from the U.S.-Israel Binational Science Foundation (2001244). Deposited in PMC for release after 12 months.

References

Adams, J. C. (1992). Biotin amplification of biotin and horseradish peroxidase signals in histochemical stains. *J. Histochem. Cytochem.* **40**, 1457-1463.
Arvanitis, D. and Davy, A. (2008). Eph/ephrin signaling: networks. *Genes Dev.* **22**, 416-429.
Bialek, P., Kern, B., Yang, X., Schrock, M., Sosic, D., Hong, N., Wu, H., Yu, K., Ornitz, D. M., Olson, E. N. et al. (2004). A twist code determines the onset of osteoblast differentiation. *Dev. Cell* **6**, 423-435.
Carver, E. A., Oram, K. F. and Gridley, T. (2002). Craniosynostosis in Twist heterozygous mice: a model for Saethre-Chotzen syndrome. *Anat. Rec.* **268**, 90-92.
Chen, L., Li, D., Li, C., Engel, A. and Deng, C. X. (2003). A Ser252Trp substitution in mouse fibroblast growth factor receptor 2 (Fgfr2) results in craniosynostosis. *Bone* **33**, 169-178.
Chen, Z. F. and Behringer, R. R. (1995). twist is required in head mesenchyme for cranial neural tube morphogenesis. *Genes Dev.* **9**, 686-699.
Cohen, M. M., Jr and MacLean, R. E. (1999). Should syndromes be defined phenotypically or molecularly? Resolution of the dilemma. *Am. J. Med. Genet.* **86**, 203-204.
Connerney, J., Andreeva, V., Leshem, Y., Muentener, C., Mercado, M. A. and Spicer, D. B. (2006). Twist1 dimer selection regulates cranial suture patterning and fusion. *Dev. Dyn.* **235**, 1345-1357.
Connerney, J., Andreeva, V., Leshem, Y., Mercado, M. A., Dowell, K., Yang, X., Lindner, V., Friesel, R. E. and Spicer, D. B. (2008). Twist1 homodimers enhance FGF responsiveness of the cranial sutures and promote suture closure. *Dev. Biol.* **318**, 323-334.
Danielian, P. S., Muccino, D., Rowitch, D. H., Michael, S. K. and McMahon, A. P. (1998). Modification of gene activity in mouse embryos in utero by a tamoxifen-inducible form of Cre recombinase. *Curr. Biol.* **8**, 1323-1326.
Deng, C., Wynshaw-Boris, A., Zhou, F., Kuo, A. and Leder, P. (1996). Fibroblast growth factor receptor 3 is a negative regulator of bone growth. *Cell* **84**, 911-921.
Dottori, M., Hartley, L., Galea, M., Paxinos, G., Polizzotto, M., Kilpatrick, T., Bartlett, P. F., Murphy, M., Kontgen, F. and Boyd, A. W. (1998). EphA4 (Sek1) receptor tyrosine kinase is required for the development of the corticospinal tract. *Proc. Natl. Acad. Sci. USA* **95**, 13248-13253.
Egea, J. and Klein, R. (2007). Bidirectional Eph-ephrin signaling during axon guidance. *Trends Cell Biol.* **17**, 230-238.
el Ghouzzi, V., Le Merrer, M., Perrin-Schmitt, F., Lajeunie, E., Benit, P., Renier, D., Bourgeois, P., Bolcato-Bellemin, A. L., Munnich, A. and Bonaventure, J. (1997). Mutations of the TWIST gene in the Saethre-Chotzen syndrome. *Nat. Genet.* **15**, 42-46.
Elowe, S., Holland, S. J., Kulkarni, S. and Pawson, T. (2001). Downregulation of the Ras-mitogen-activated protein kinase pathway by the EphB2 receptor tyrosine kinase is required for ephrin-induced neurite retraction. *Mol. Cell. Biol.* **21**, 7429-7441.
Feldheim, D. A., Kim, Y. I., Bergemann, A. D., Frisen, J., Barbacid, M. and Flanagan, J. G. (2000). Genetic analysis of ephrin-A2 and ephrin-A5 shows their requirement in multiple aspects of retinocollicular mapping. *Neuron* **25**, 563-574.
Guenou, H., Kaabeche, K., Mee, S. L. and Marie, P. J. (2005). A role for fibroblast growth factor receptor-2 in the altered osteoblast phenotype induced by Twist haploinsufficiency in the Saethre-Chotzen syndrome. *Hum. Mol. Genet.* **14**, 1429-1439.
Howard, T. D., Paznekas, W. A., Green, E. D., Chiang, L. C., Ma, N., Ortiz de Luna, R. I., Garcia Delgado, C., Gonzalez-Ramos, M., Kline, A. D. and Jabs, E. W. (1997). Mutations in TWIST, a basic helix-loop-helix transcription factor, in Saethre-Chotzen syndrome. *Nat. Genet.* **15**, 36-41.
Ishii, M., Merrill, A. E., Chan, Y. S., Gitelman, I., Rice, D. P., Sucov, H. M. and Maxson, R. E., Jr (2003). Msx2 and Twist cooperatively control the development of the neural crest-derived skeletogenic mesenchyme of the murine skull vault. *Development* **130**, 6131-6142.
Jabs, E. W., Muller, U., Li, X., Ma, L., Luo, W., Haworth, I. S., Klisak, I., Sparkes, R., Warman, M. L., Mulliken, J. B. et al. (1993). A mutation in the homeodomain of the human MSX2 gene in a family affected with autosomal dominant craniosynostosis. *Cell* **75**, 443-450.
Jabs, E. W., Li, X., Scott, A. F., Meyers, G., Chen, W., Eccles, M., Mao, J. I., Charnas, L. R., Jackson, C. E. and Jaye, M. (1994). Jackson-Weiss and Crouzon syndromes are allelic with mutations in fibroblast growth factor receptor 2. *Nat. Genet.* **8**, 275-279.
Jenkins, D., Seelow, D., Jehee, F. S., Perlyn, C. A., Alonso, L. G., Bueno, D. F., Donnai, D., Josifova, D., Mathijssen, I. M., Morton, J. E. et al. (2007). RAB23 mutations in Carpenter syndrome imply an unexpected role for hedgehog signaling in cranial-suture development and obesity. *Am. J. Hum. Genet.* **80**, 1162-1170.
Jiang, X., Choudhary, B., Merki, E., Chien, K. R., Maxson, R. E. and Sucov, H. M. (2002). Normal fate and altered function of the cardiac neural crest cell lineage in retinoic acid receptor mutant embryos. *Mech. Dev.* **117**, 115-122.
Johnson, D., Iseki, S., Wilkie, A. O. and Morriss-Kay, G. M. (2000). Expression patterns of Twist and Fgfr1, -2 and -3 in the developing mouse coronal suture suggest a key role for twist in suture initiation and biogenesis. *Mech. Dev.* **91**, 341-345.
Kim, H. J., Rice, D. P., Kettunen, P. J. and Thesleff, I. (1998). FGF-, BMP- and Shh-mediated signalling pathways in the regulation of cranial suture morphogenesis and calvarial bone development. *Development* **125**, 1241-1251.
Klein, R. (2004). Eph/ephrin signaling in morphogenesis, neural development and plasticity. *Curr. Opin. Cell Biol.* **16**, 580-589.
Kullander, K. and Klein, R. (2002). Mechanisms and functions of Eph and ephrin signalling. *Nat. Rev. Mol. Cell Biol.* **3**, 475-486.
Lana-Elola, E., Rice, R., Grigoriadis, A. E. and Rice, D. P. (2007). Cell fate specification during calvarial bone and suture development. *Dev. Biol.* **311**, 335-346.
Lee, M. S., Lowe, G. N., Strong, D. D., Wergedal, J. E. and Glackin, C. A. (1999). TWIST, a basic helix-loop-helix transcription factor, can regulate the human osteogenic lineage. *J. Cell. Biochem.* **75**, 566-577.
Liu, B., Yu, H. M. and Hsu, W. (2007). Craniosynostosis caused by Axin2 deficiency is mediated through distinct functions of beta-catenin in proliferation and differentiation. *Dev. Biol.* **301**, 298-308.
Marie, P. J., Coffin, J. D. and Hurley, M. M. (2005). FGF and FGFR signaling in chondrodysplasias and craniosynostosis. *J. Cell. Biochem.* **96**, 888-896.
Martinez, A. and Soriano, E. (2005). Functions of ephrin/Eph interactions in the development of the nervous system: emphasis on the hippocampal system. *Brain Res. Brain Res. Rev.* **49**, 211-226.
Maxson, R. and Ishii, M. (2008). The Bmp pathway in skull vault development. *Front. Oral Biol.* **12**, 197-208.
Merrill, A. E., Bochukova, E. G., Brugger, S. M., Ishii, M., Pilz, D. T., Wall, S. A., Lyons, K. M., Wilkie, A. O. and Maxson, R. E., Jr (2006). Cell mixing at a neural crest-mesoderm boundary and deficient ephrin-Eph signaling in the pathogenesis of craniosynostosis. *Hum. Mol. Genet.* **15**, 1319-1328.
Meyers, G. A., Orlow, S. J., Munro, I. R., Przylepa, K. A. and Jabs, E. W. (1995). Fibroblast growth factor receptor 3 (FGFR3) transmembrane mutation in Crouzon syndrome with acanthosis nigricans. *Nat. Genet.* **11**, 462-464.
Miao, H., Wei, B. R., Peehl, D. M., Li, Q., Alexandrou, T., Schelling, J. R., Rhim, J. S., Sedor, J. R., Burnett, E. and Wang, B. (2001). Activation of EphA receptor tyrosine kinase inhibits the Ras/MAPK pathway. *Nat. Cell Biol.* **3**, 527-530.
Muneoka, K., Wanek, N. and Bryant, S. V. (1986). Mouse embryos develop normally exo utero. *J. Exp. Zool.* **239**, 289-293.
Nieto, M. A., Gilardi-Hebenstreit, P., Charnay, P. and Wilkinson, D. G. (1992). A receptor protein tyrosine kinase implicated in the segmental patterning of the hindbrain and mesoderm. *Development* **116**, 1137-1150.
Ornitz, D. M. and Marie, P. J. (2002). FGF signaling pathways in endochondral and intramembranous bone development and human genetic disease. *Genes Dev.* **16**, 1446-1465.
Palmer, A. and Klein, R. (2003). Multiple roles of ephrins in morphogenesis, neuronal networking, and brain function. *Genes Dev.* **17**, 1429-1450.
Paratore, C., Suter, U. and Sommer, L. (1999). Embryonic gene expression resolved at the cellular level by fluorescence in situ hybridization. *Histochem. Cell Biol.* **111**, 435-443.
Pasquale, E. B. (2005). Eph receptor signalling casts a wide net on cell behaviour. *Nat. Rev. Mol. Cell Biol.* **6**, 462-475.
Pasquale, E. B. (2008). Eph-ephrin bidirectional signaling in physiology and disease. *Cell* **133**, 38-52.
Poliakov, A., Cotrina, M. and Wilkinson, D. G. (2004). Diverse roles of eph receptors and ephrins in the regulation of cell migration and tissue assembly. *Dev. Cell* **7**, 465-480.

Pratt, R. L. and Kinch, M. S. (2002). Activation of the EphA2 tyrosine kinase stimulates the MAP/ERK kinase signaling cascade. *Oncogene* **21**, 7690-7699.
Rawlins, J. T. and Opperman, L. A. (2008). Tgf-beta regulation of suture morphogenesis and growth. *Front. Oral Biol.* **12**, 178-196.
Rice, D. P., Kim, H. J. and Thesleff, I. (1999). Apoptosis in murine calvarial bone and suture development. *Eur. J. Oral Sci.* **107**, 265-275.
Rice, D. P., Aberg, T., Chan, Y., Tang, Z., Kettunen, P. J., Pakarinen, L., Maxson, R. E. and Thesleff, I. (2000). Integration of FGF and TWIST in calvarial bone and suture development. *Development* **127**, 1845-1855.
Ryoo, H. M., Lee, M. H. and Kim, Y. J. (2006). Critical molecular switches involved in BMP-2-induced osteogenic differentiation of mesenchymal cells. *Gene* **366**, 51-57.
Saga, Y., Miyagawa-Tomita, S., Takagi, A., Kitajima, S., Miyazaki, J. and Inoue, T. (1999). MesP1 is expressed in the heart precursor cells and required for the formation of a single heart tube. *Development* **126**, 3437-3447.
Santiago, A. and Erickson, C. A. (2002). Ephrin-B ligands play a dual role in the control of neural crest cell migration. *Development* **129**, 3621-3632.
Schmucker, D. and Zipursky, S. L. (2001). Signaling downstream of Eph receptors and ephrin ligands. *Cell* **105**, 701-704.
Serbedzija, G. N., Bronner-Fraser, M. and Fraser, S. E. (1992). Vital dye analysis of cranial neural crest cell migration in the mouse embryo. *Development* **116**, 297-307.
Shukla, V., Coumoul, X., Wang, R. H., Kim, H. S. and Deng, C. X. (2007). RNA interference and inhibition of MEK-ERK signaling prevent abnormal skeletal phenotypes in a mouse model of craniosynostosis. *Nat. Genet.* **39**, 1145-1150.
Soriano, P. (1999). Generalized lacZ expression with the ROSA26 Cre reporter strain. *Nat. Genet.* **21**, 70-71.
Surawska, H., Ma, P. C. and Salgia, R. (2004). The role of ephrins and Eph receptors in cancer. *Cytokine Growth Factor Rev.* **15**, 419-433.
Vindis, C., Cerretti, D. P., Daniel, T. O. and Huynh-Do, U. (2003). EphB1 recruits c-Src and p52Shc to activate MAPK/ERK and promote chemotaxis. *J. Cell Biol.* **162**, 661-671.
Wang, Y., Xiao, R., Yang, F., Karim, B. O., Iacovelli, A. J., Cai, J., Lerner, C. P., Richtsmeier, J. T., Leszl, J. M., Hill, C. A. et al. (2005). Abnormalities in cartilage and bone development in the Apert syndrome FGFR2(+/S252W) mouse. *Development* **132**, 3537-3548.
Wang, X., Roy, P. J., Holland, S. J., Zhang, L. W., Culotti, J. G. and Pawson, T. (1999). Multiple ephrins control cell organization in C. elegans using kinase-dependent and -independent functions of the VAB-1 Eph receptor. *Mol. Cell* **4**, 903-913.
Warren, S. M., Brunet, L. J., Harland, R. M., Economides, A. N. and Longaker, M. T. (2003). The BMP antagonist noggin regulates cranial suture fusion. *Nature* **422**, 625-629.
Wilkie, A. O. (1997). Craniosynostosis: genes and mechanisms. *Hum. Mol. Genet.* **6**, 1647-1656.
Wilkie, A. O. and Morriss-Kay, G. M. (2001). Genetics of craniofacial development and malformation. *Nat. Rev Genet.* **2**, 458-468.
Wilkinson, D. G. (2001). Multiple roles of EPH receptors and ephrins in neural development. *Nat. Rev. Neurosci.* **2**, 155-164.
Yamaguchi, T. P. and Rossant, J. (1995). Fibroblast growth factors in mammalian development. *Curr. Opin. Genet. Dev.* **5**, 485-491.
Yang, H., Wanner, I. B., Roper, S. D. and Chaudhari, N. (1999). An optimized method for in situ hybridization with signal amplification that allows the detection of rare mRNAs. *J. Histochem. Cytochem.* **47**, 431-446.
Yin, L., Du, X., Li, C., Xu, X., Chen, Z., Su, N., Zhao, L., Qi, H., Li, F., Xue, J. et al. (2008). A Pro253Arg mutation in fibroblast growth factor receptor 2 (Fgfr2) causes skeleton malformation mimicking human Apert syndrome by affecting both chondrogenesis and osteogenesis. *Bone* **42**, 631-643.
Yoshida, T. (2005). Growth pattern of the frontal bone primordium and involvement of Bmps in this process. *Kokubyo Gakkai Zasshi* **72**, 19-27.
Yoshida, T., Phylactou, L. A., Uney, J. B., Ishikawa, I., Eto, K. and Iseki, S. (2005). Twist is required for establishment of the mouse coronal suture. *J. Anat.* **206**, 437-444.
Yoshida, T., Vivatbutsiri, P., Morriss-Kay, G., Saga, Y. and Iseki, S. (2008). Cell lineage in mammalian craniofacial mesenchyme. *Mech. Dev.* **125**, 797-808.
Yousfi, M., Lasmoles, F., Lomri, A., Delannoy, P. and Marie, P. J. (2001). Increased bone formation and decreased osteocalcin expression induced by reduced Twist dosage in Saethre-Chotzen syndrome. *J. Clin. Invest.* **107**, 1153-1161.
Yousfi, M., Lasmoles, F., El Ghouzzi, V. and Marie, P. J. (2002). Twist haploinsufficiency in Saethre-Chotzen syndrome induces calvarial osteoblast apoptosis due to increased TNFalpha expression and caspase-2 activation. *Hum. Mol. Genet.* **11**, 359-369.
Yu, H. M., Jerchow, B., Sheu, T. J., Liu, B., Costantini, F., Puzas, J. E., Birchmeier, W. and Hsu, W. (2005). The role of Axin2 in calvarial morphogenesis and craniosynostosis. *Development* **132**, 1995-2005.
Yu, K., Xu, J., Liu, Z., Sosic, D., Shao, J., Olson, E. N., Towler, D. A. and Ornitz, D. M. (2003). Conditional inactivation of FGF receptor 2 reveals an essential role for FGF signaling in the regulation of osteoblast function and bone growth. *Development* **130**, 3063-3074.